Oil Shale, 2017, Vol. 34, No. 3, pp. 197–218
doi: https//doi.org/10.3176/oil.2017.3.01
ISSN 0208-189X

ORGANIC GEOCHEMICAL STUDY OF THE UPPER LAYER OF ALEKSINAC OIL SHALE IN THE DUBRAVA BLOCK, SERBIA

GORDANA GAJICA[(a)*], ALEKSANDRA ŠAJNOVIĆ[(a)], KSENIJA STOJANOVIĆ[(b)], ALEKSANDAR KOSTIĆ[(c)], IAN SLIPPER[(d)], MILAN ANTONIJEVIĆ[(d)], HANS PETER NYTOFT[(e)], BRANIMIR JOVANČIĆEVIĆ[(b)]

[(a)] University of Belgrade, Institute of Chemistry, Technology and Metallurgy, Center of Chemistry, Studentski trg 12–16, 11000 Belgrade, Serbia
[(b)] University of Belgrade, Faculty of Chemistry, Studentski trg 12–16, 11000 Belgrade, Serbia
[(c)] University of Belgrade, Faculty of Mining and Geology, Đušina 7, 11000 Belgrade, Serbia
[(d)] University of Greenwich, Faculty of Engineering & Science, Central Avenue, Chatham, ME4 4TB, United Kingdom
[(e)] Geological Survey of Denmark and Greenland, Øster Voldgade 10, DK-1350, Copenhagen, Denmark

Abstract. *A detailed evaluation of geochemical properties of oil shale samples from the outcrops of the Lower Miocene upper layer in the Dubrava area, Aleksinac basin, Serbia, was performed. For that purpose X-ray diffraction (XRD) analysis, Rock Eval pyrolysis, gas chromatography-mass spectrometry (GC-MS) analysis of biomarkers and conventional pyrolysis in an autoclave were used.*

Most of the samples have similar mineral compositions with predominance of clay and feldspar minerals. Three samples are characterised by an elevated content of carbonates, and among them one sample has a notable prevalence of this mineral group. This sample also demonstrated certain differences in biomarker distribution.

In most samples organic matter (OM) consists predominantly of type I and II kerogens, showing high oil generative potential, whereas three samples, which contain type II kerogen with a certain input of type III kerogen, demonstrated potential to produce both, oil and gas. The OM of all samples is immature and corresponds to the vitrinite reflectance of ca. 0.40%. Biomarker patterns along with Rock-Eval data indicated a strong contribution of aquatic organisms such as green and brown algae and bacteria with some influence of higher plants OM. The organic matter was deposited in a reducing lacustrine alkaline brackish to freshwater environment under warm

[*] Corresponding author: e-mail: *ggajica@chem.bg.ac.rs*

climate conditions. Preservation of OM was governed by stratification of the water column rather than its height. Tectonic movements that caused the regional tilting of an investigated area and supported minor marine ingression and influx of fresh water played an important role in formation of the sediments.

Conventional pyrolytic experiments confirmed that these sediments at the catagenetic stage could be a significant source of liquid hydrocarbons.

***Keywords**: mineral composition, hydrocarbon potential, biomarkers, pyrolysis, Aleksinac oil shale, Serbia.*

1. Introduction

Twenty discoveries and two deposits of oil shale (OS) of Cenozoic age, mostly of the Neogene, have been found in Serbia. However, the majority of these accumulations with variable kerogen content and oil yield have been poorly explored. Aleksinac is the largest, richest and most thoroughly explored oil shale deposit in Serbia. The total estimated oil shale resources of Serbia are ca. 5 billion tons, while the potential reserves of the Aleksinac deposit are estimated at ca. 2.1 billion tons [1, 2].

During the last few decades the Aleksinac oil shale has been studied with the focus on both, fundamental and applied aspects [1–6]. However, a detailed organic geochemical examination of the oil shale has not been performed.

Organic matter (OM) is usually present in small amounts in sedimentary rocks like oil shale. Nevertheless it can provide important information about the origin, depositional environment, including climate, as well as age and maturity of oil shale. Also oil and gas generative potential of oil shale depends on the quantity, type and maturity of OM [7, 8]. For a better evaluation of the hydrocarbon potential of an immature OS sample, simulation of OM maturity changes in laboratory conditions by pyrolysis is commonly used [9, 10]. As the largest part of the sedimentary rocks is inorganic matter, analysis of OS mineral composition is important for the evaluation of depositional environment and effects of minerals on the OM preservation [7].

For this investigation, oil shale samples from the outcrops of the Lower Miocene upper layer in the Dubrava area were collected. The aim of this study is to provide a detailed evaluation of geochemical properties of the Aleksinac oil shale with the purpose of determining the quantity, type, depositional environment, thermal maturity and hydrocarbon generative potential of its OM.

2. Geological setting

The Aleksinac oil shale deposit is located about 200 km southeast from Belgrade, in the Kruševac-Aleksinac Cenozoic basin (see Fig. 4 in [2]). It

covers an area of over 13 km^2, with the resources of oil shale of ca. 2.1 billion tons [1]. The deposit is filled by Lower and Upper Miocene sediments. The Lower Miocene lacustrine sediments are up to 800 m thick. The basal conglomerates are overlain by alluvial-lacustrine sandstones, with some sandy shale and siltstone in the upper layers (Fig. 1). These sediments are overlain by two layers of oil shale, and the main coal seam is located between them (2–6 m thick, locally up to 15 m) [3]. The Lower Miocene complex is covered by a layer of up to 700 m thick Upper Miocene marl, clay, sand and conglomerate (Fig. 2) [11].

The lower oil shale layer has an average net thickness of approximately 20 m, and besides interburden sediments there are some thin coal layers. The upper oil shale layer has an average net thickness of approximately 56 m and directly covers the main coal seam (Fig. 2). Outcrops of both coal and oil shale, which are in direct contact, are exposed on the surface in the area of an abandoned open-pit mine.

In the Aleksinac oil shale kerogen type I predominates, with more than 80 vol% [3, 12]. The kerogen mainly consists of degraded alginite with a characteristic laminated microtexture (lamalginite), rarely of telalginite. A relatively small percentage of kerogen type II (sporinite, liptodetrinite) was observed, while coaly kerogen was very sparse (< 4 vol%). An average oil yield (Fischer assay) of the upper layer of the Aleksinac oil shale is 8.5% [3].

The Aleksinac deposit has a very complex tectonic setting as a result of large tectonic movements, which caused crimping, horizontal movements and numerous faults. By the end of the Lower Miocene, a steady lacustrine phase was terminated by intensive folding and faulting in the area, and the

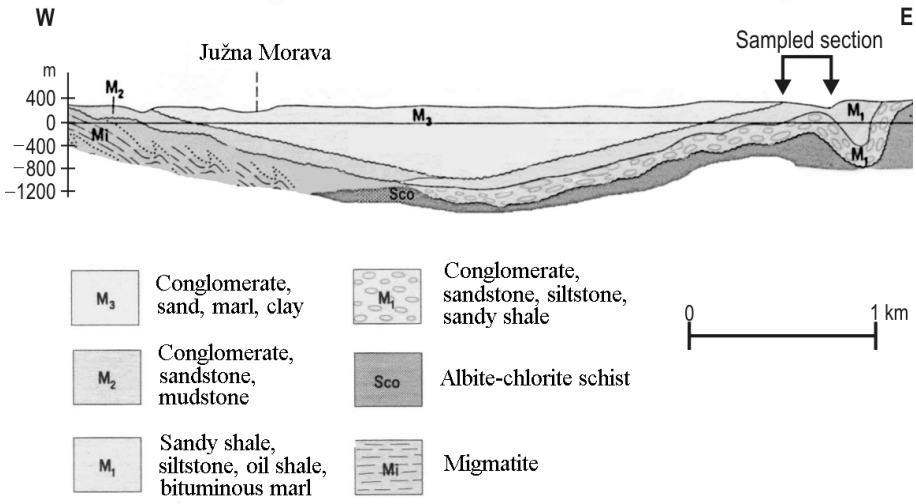

Fig. 1. Cross-section of the Kruševac-Aleksinac basin, with marked sampled outcrop section (on the right).

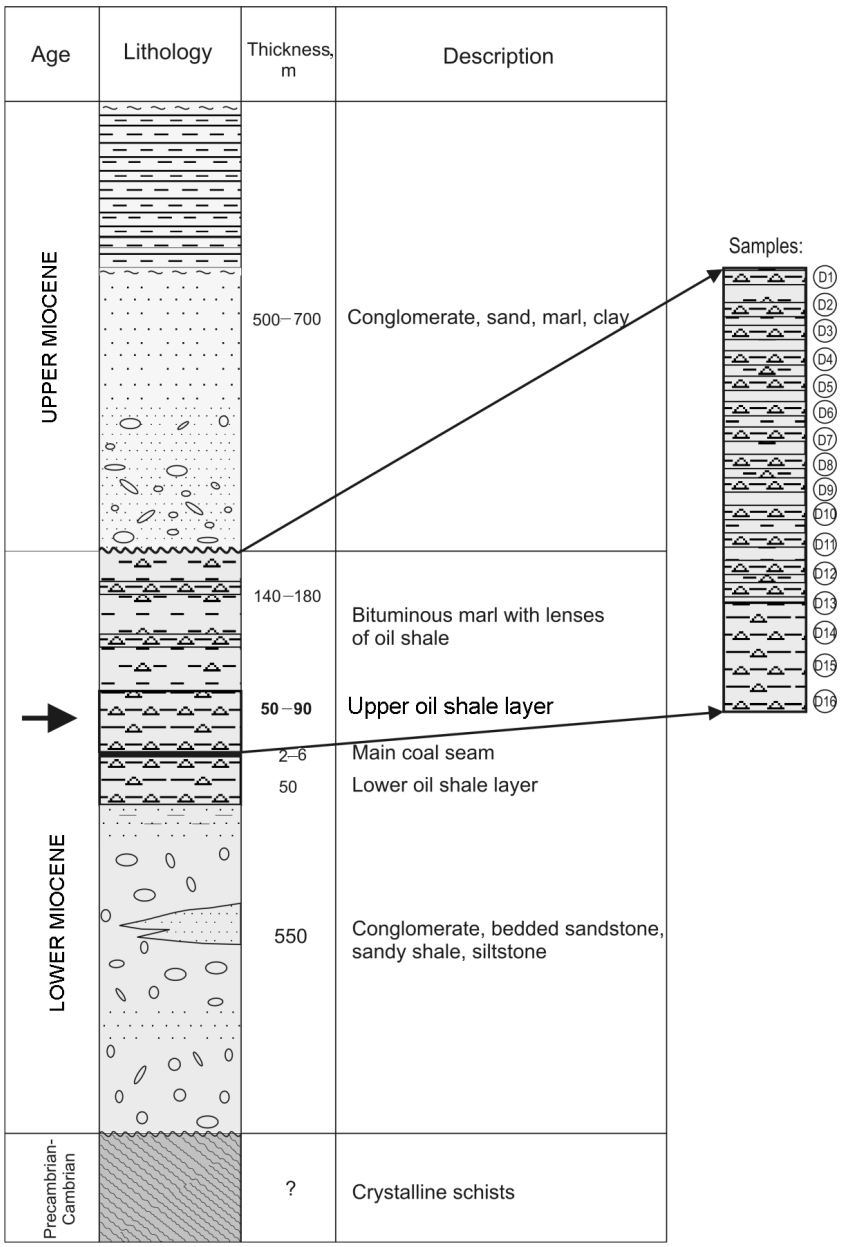

Fig. 2. Geological column of the Aleksinac deposit area, with position of samples D1–D16.

deposit was divided into tectonic blocks, with significant dipping angles [11]. The north-south trending belt of the Aleksinac oil shale deposit is divided by fault zones into three major blocks: Dubrava, Morava and Logorište. Minor faults divide the fields into numerous smaller blocks, from

hectometer to kilometer in size. Offsets of layers in faults zones amount to 100 m, which causes the discontinuity of oil shale seams [11].

For the purpose of this study, sixteen samples were taken in the Dubrava block, from the outcropping upper layer of Lower Miocene oil shale, precisely from a 250 m thick sequence above the main coal seam. The samples were taken as discontinuous channel samples, from the top of the bituminous marl sequence to the bottom of the upper oil shale layer (Fig. 2).

3. Analytical methods

Rock-Eval pyrolysis was performed using a Rock-Eval 6 Standard analyser. About 25 mg of pulverized sample (fraction 0.2–0.4 mm) was used for the analysis. IPF 160000 calibration sample was used as the standard.

Procedures for elemental analysis, isolation of extractable OM (bitumen) and separation of saturated, aromatic and polar (nitrogen, sulphur, and oxygen, NSO-compounds) fractions from bitumen, as well as gas chromatography-mass spectrometry (GC-MS) which was used for analyses of biomarkers, were explained in detail in our previous papers [13, 14].

The pyrolysis was performed on selected extracted (bitumen-free) sample containing kerogen with native minerals. The process was carried out in an autoclave under a nitrogen atmosphere, for 4 h at a temperature of 400 °C. Liquid pyrolysis products were extracted with hot chloroform. The liquid pyrolysates were further treated using the same methods applied to bitumen extracted from the oil shale samples (see above).

X-ray diffraction (XRD) was used for mineral identification and quantification. The XRD analysis was conducted on a Bruker D8-Advance diffractometer equipped with a Cu anode tube at 40 kV and 40 mA. The samples were analysed in the scan range from 2° to 70° (2θ), with a step size of 0.02° (2θ) and a counting time of 1 second per step. A LynxEye silicon strip position sensitive detector was used with a 3° opening and 176 active channels; the effective counting time was therefore 176 seconds per step. The sample rotation speed was 15 rpm. The data were collected by DIFFRAC-Plus Commander v.2.6.1 software (Bruker-AXS), and qualitative analysis was done using EVA v.16 (Bruker-AXS) and PDF-2 database (ICDD, 2008) [15]. Quantification was performed using TOPAS Rietveld refinement software (Bruker-AXS).

4. Results and discussion

4.1. Mineral composition

The mineral part of analysed samples is composed of clays, feldspars, carbonates, analcime, natrolite, quartz and bassanite (Table 1). Clay and feldspar minerals dominate in most of the samples, while sample D16 has a high content of carbonates (Table 1). Clay minerals are mostly composed

Table 1. Semi-quantitative mineral composition from Rietveld refinement (expressed as a percent of total mineral matter, excluding mixed layer clay)

Mineral	Sample No.															
	D1	D2	D3	D4	D5	D6	D7	D8	D9	D10	D11	D12	D13	D14	D15	D16
Analcime	18.70	10.76	10.22	33.53	11.96	8.69	14.54	10.47	10.11	8.10	13.50	15.5	15.13	15.6	20.3	NI
Natrolite	0.64	1.14	2.42	2.80	2.69	1.37	1.11	0.74	0.96	0.37	0.48	0.78	0.56	1.73	0.43	NI
Quartz	NI	13.09	3.33	0.48	10.15	NI	NI	4.70	3.92	4.06	6.34	4.80	10.51	5.40	5.00	2.75
Bassanite	NI	NI	NI	NI	NI	NI	NI	NI	NI	NI	NI	NI	NI	NI	NI	1.41
Microcline	15.20	6.90	25.76	19.10	5.42	26.20	17.36	19.00	18.40	17.00	15.00	14.10	4.99	14.40	10.20	NI
Orthoclase	NI	4.09	2.01	3.81	23.61	NI	NI	NI	0.98	0.93	0.87	0.70	1.41	3.30	4.60	NI
Sanidine	NI	NI	NI	3.19	5.10	NI	NI	NI	2.36	1.91	1.25	1.10	NI	NI	NI	NI
Albite	6.32	8.93	8.64	4.85	5.18	4.74	5.41	6.84	10.69	9.80	8.00	7.82	4.83	7.80	5.20	NI
Total feldspars	21.50	20.73	36.41	30.95	39.31	31.00	22.77	25.84	32.43	29.60	25.12	23.72	11.23	25.50	20.00	NI
Dolomite	7.58	24.00	10.31	9.31	20.10	9.57	8.56	14.65	4.19	12.00	11.4	12.30	24.90	14.7	17.00	NI
Ca-rich dolomite (or ankerite)	NI	13.50	12.89	NI	NI	NI	NI	NI	3.14	6.00	4.10	6.50	9.05	7.10	5.90	NI
Calcite	2.42	NI	1.02	NI	NI	4.74	NI	6.54	NI	NI	1.92	4.77	NI	NI	4.20	17.09
Aragonite	NI	NI	NI	NI	NI	NI	NI	NI	NI	NI	NI	NI	NI	NI	NI	46.78
Total carbonates	10.00	37.50	24.22	9.31	20.10	14.30	8.56	21.19	7.33	18.00	17.42	23.57	33.95	21.80	27.10	63.87
Muscovite	32.60	10.21	12.38	11.8	12.65	30.00	38.60	26.40	29.60	26.00	25.00	19.00	19.2	17.00	19.00	24.18
Chlorite	3.64	4.02	7.74	6.97	NI	2.57	2.35	3.44	3.59	1.04	3.14	1.31	0.31	4.90	7.80	NI
Smectite	13.00	2.61	3.29	4.17	3.11	12.1	12.02	7.13	12.10	12.80	8.60	11.37	9.16	8.50	NI	6.39
Kaolinite	NI	NI	NI	NI	NI	NI	NI	NI	NI	NI	NI	NI	NI	NI	NI	1.40
Total clays	49.20	16.84	23.41	22.94	15.76	44.70	52.97	36.97	45.29	39.80	36.74	31.68	28.67	30.40	26.80	31.97

NI – not identified.

of muscovite, followed by smectite and chlorite, while kaolinite is present only in sample D16 (Table 1). Feldspars are mainly represented by microcline and albite, followed by orthoclase and sanidine in some samples (Table 1). Their presence could indicate the terrigenous influence.

Carbonate minerals are identified in all samples. Dolomite is present in all samples with the exception of sample D16 (Table 1). Some samples contain Ca-rich dolomite (or ankerite) and calcite, while aragonite is present exclusively in sample D16 as a dominant mineral (Table 1). Calcite and aragonite are of biogenic and/or chemical origin. While calcite can arise in different environments, aragonite usually occurs in the warm, shallow marine environment with reduced salinity, formed by direct precipitation from seawater or from skeletons of various organisms [16]. According to Müller et al. [17] it is formed in alkaline saline lakes.

Quartz is identified in almost all investigated samples in relatively low amount (Table 1). Quartz, feldspars and carbonates are regarded as brittle minerals which have an important effect on the shale fragility [18].

Minerals of the zeolite group, analcime and natrolite, are present in all samples except in sample D16 (Table 1). Analcime was found in saline lakes and terrestrial sediments in warm, rather arid regions, frequently associated with phillipsite, chabazite and natrolite [19]. Analcime often occurs in sedimentary lacustrine basins in association with volcanoclastic material. Since pronounced volcanic activity during the Miocene in the area of the Aleksinac deposit was documented [20], the presence of this mineral in analysed samples was expected.

Bassanite is present only in sample D16 (Table 1). It is formed via dehydration of gypsum at higher temperatures. Additionally, bassanite can be formed as a primary evaporite mineral in a higher temperature setting or by evaporation of highly saline solutions [21].

Mineral analysis has shown that samples D1–D15 have almost the same constituents, while sample D16 has a different composition. This result indicates certain changes in the depositional environment during formation of samples D16 and D1–D15.

4.2. Organic geochemistry of investigated samples

4.2.1. General characteristics

Total organic carbon (TOC) ranges from 1.31 to 29.10 wt%, being notably higher in D16 than in other samples (Table 2). The content of free and weakly adsorbed hydrocarbons (S1) is in the range of 0.07–2.85 mg HC/g rock (Table 2). The S1/TOC ratio shows that free hydrocarbons (HC) of investigated samples are indigenous and there is no organic contamination [22]. The content of bitumen in analysed samples ranges from 1565 to 16239 ppm, and as TOC is considerably higher in sample D16 (Table 2). The content of HC in bitumen is in the range of 9.27–24.00 wt% (Table 2).

Table 2. Rock-Eval data and group organic geochemical parameters

Sample No.	Litho-logy	C_{org}	TS	TOC	S1	S2	S3	T_{max}	HI	PI	OI	S2/S3	PY	PC	RC	Bitumen	HC
D1	BM	3.25	0.13	2.85	0.19	18.59	2.12	439	652	0.01	74	8.77	18.78	1.58	1.27	1565	13.73
D2	OS	6.29	0.21	7.06	0.50	52.03	3.85	438	737	0.01	55	13.51	52.53	4.56	2.50	3429	19.33
D3	BM	4.07	0.18	3.87	0.26	24.63	2.38	437	636	0.01	61	10.35	24.89	2.19	1.68	4398	20.00
D4	BM	1.98	0.13	1.79	0.11	8.13	1.83	437	454	0.01	102	4.44	8.24	0.77	1.02	2877	20.67
D5	OS	5.15	0.23	5.44	0.28	38.36	3.09	439	705	0.01	57	12.41	38.64	3.37	2.07	4337	13.91
D6	BM	1.41	0.13	1.31	0.07	5.24	1.36	444	400	0.02	104	3.85	5.31	0.51	0.80	1717	13.70
D7	BM	1.95	0.13	1.88	0.14	8.62	1.65	440	459	0.01	88	5.22	8.76	0.81	1.07	2259	24.00
D8	OS	5.49	0.15	5.20	0.31	37.85	2.85	439	728	0.01	55	13.28	38.16	3.31	1.89	3257	16.56
D9	OS	5.52	0.09	5.10	0.32	35.46	2.81	439	695	0.01	55	12.62	35.78	3.11	1.99	3521	16.00
D10	OS	8.57	0.08	8.22	0.38	64.17	4.14	439	781	0.01	50	15.50	64.55	5.57	2.65	4008	9.27
D11	BM	3.64	0.07	3.83	0.21	23.75	2.42	437	620	0.01	63	9.81	23.96	2.13	1.70	4827	13.25
D12	OS	7.25	0.08	7.20	0.43	53.81	3.88	440	747	0.01	54	13.87	54.24	4.70	2.50	2837	19.33
D13	OS	12.88	0.21	13.10	1.90	112.34	4.29	443	858	0.02	33	26.19	114.24	9.72	3.38	6589	9.87
D14	BM	3.78	0.06	4.01	0.32	25.17	2.09	438	628	0.01	52	12.04	25.49	2.23	1.78	3504	19.21
D15	OS	7.94	0.14	8.61	0.76	63.88	3.93	439	742	0.01	46	16.25	64.64	5.59	3.02	4491	10.53
D16	OS	32.85	6.11	29.10	2.85	180.10	9.03	436	619	0.02	31	19.94	182.92	18.50	10.60	16239	13.16
Minimum		1.41	0.06	1.31	0.07	5.24	1.36	436	400	0.01	31	3.85	5.31	0.51	0.80	1565	9.27
Maximum		32.85	6.11	29.10	2.85	180.10	9.03	444	858	0.02	104	26.19	182.92	18.50	10.60	16239	24.00
Average		7.00	0.51	6.79	0.56	47.01	3.23	439	654	0.01	61	12.38	47.57	4.35	2.43	4366	15.78

Note: BM – bituminous marlstone; OS – oil shale; C_{org} – content of organic carbon, wt%, obtained by elemental analysis; TS – total content of sulphur, wt%; TOC – total organic carbon, wt%, obtained by Rock-Eval pyrolysis; S1 – free hydrocarbons, mg HC/g rock; S2 – pyrolysate hydrocarbons, mg HC/g rock; S3 – amount of CO_2 generated from oxygenated functional groups, mg CO_2/g rock; T_{max} – temperature corresponding to S_2 peak maximum, ºC; HI – Hydrogen Index = (S2 × 100)/TOC, mg HC/g TOC; PI – Production Index = S1/(S1 + S2); OI – Oxygen Index = (S3 × 100)/TOC, mg CO_2/g TOC; PY – hydrocarbon generative potential or potential yield = S1 + S2, kg HC/t rock; PC – pyrolysable carbon, wt%; RC – residual carbon, wt%; bitumen – content of bitumen, ppm; HC – content of hydrocarbons in bitumen, wt%.

The kerogen type, or quality of OM, was determined by diagrams Hydrogen Index (HI) vs maximal temperature (T_{max}) and HI vs Oxygen Index (OI) (Fig. 3) [7, 23], as well as by the S2 /S3 ratio (Table 2). According to the mentioned diagrams, OM of the majority of the samples comprises type I and II kerogens. The OM of sample D13 consists predominantly of type I kerogen, whereas that of samples D4, D6 and D7 is dominated by type II kerogen (Fig. 3). The S2/S3 ratio higher than 5 mg HC/mg CO_2 (Table 2) indicates that most of the samples contain type I or II kerogen. The lowest values of this parameter are observed for samples D4, D6 and D7, implying contribution of type III kerogen [24, 25].

Production Index (PI) values in the range of 0.01–0.02 (Table 2) indicate an immature stage. PI also reveals that there is no external contribution of migrated hydrocarbons to the organic-rich facies, which is in agreement with values of S1. T_{max} is in the range from 436 to 444 °C (Table 2). T_{max} is not a reliable maturity indicator since its value depends on kerogen type [9, 24, 26]. Considering that most of the samples have a significant contribution of kerogen I type (Fig. 3), the obtained T_{max} values indicate that the investigated samples are in the immature to early mature stage [7, 24].

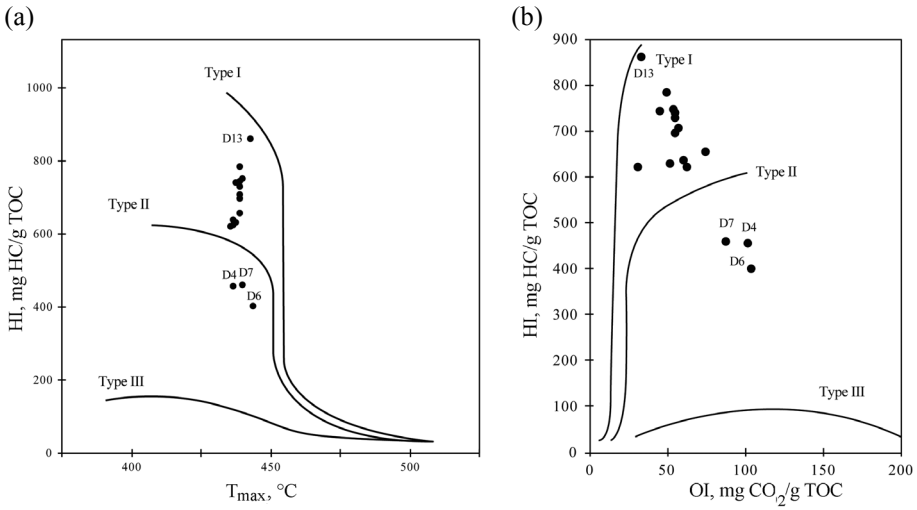

Fig. 3. HI vs T_{max} (a) and HI vs OI (b) diagrams.

4.2.2. Hydrocarbon generative potential

Since the OM of all samples is immature to early mature, the hydrocarbon generative potential predominantly depends on its quantity and type. As mentioned in the previous section, the OM of all samples is dominated by type I and II kerogens or a mixture of these two, which have a high hydrogen content and therefore a high potential for hydrocarbon generation. Otherwise, the S2/S3 ratio (Table 2) shows that samples D4, D6 and D7 contain a certain amount of lower quality OM, type III kerogen depleted in hydrogen.

Pyrolysable carbon (PC) corresponds to the carbon present in the HC represented by S1 and S2. PC × 100/TOC value > 30% indicates an oil prone source rock [26]. In analysed samples TOC mostly consists of PC with an average value about 60% of TOC (Table 2), indicating that the samples have a high hydrocarbon generative potential. Residual carbon (RC) is generally low in investigated samples (Table 2).

Based on the pyrolysable hydrocarbons, S2 > 20 mg HC/g rock (Table 2), the majority of the samples have an excellent source rock potential, whereas samples D4, D6 and D7 show a good source rock potential (Table 2) [23, 27]. Hydrocarbon generative potential (PY) value represents the maximum quantity of HC that a sufficiently matured source rock might generate [26]. All samples have PY values > 2 kg HC/t of rock (Table 2) which can be considered as a prerequisite for classification as a possible oil source rock [22]. Based on PY values (Table 2), most of the samples have an excellent generative potential for oil, D4 and D7 samples have a good, and only sample D6 has a fair to good generative potential [28].

The HI values in the range of 400–858 mg HC/g TOC (Table 2) indicate that the kerogen is oil prone with a high potential for oil generation [25]. The plot T_{max} vs HI (Fig. 4) implies that almost all samples have potential to generate oil, whereas three samples – D4, D6, D7, have potential to generate both oil and gas.

Based on Rock-Eval parameters and corresponding diagrams all samples showed a high generative potential for oil, with exception of samples D4, D6 and D7 which have potential to produce both, oil and gas. This is consistent with the estimated kerogen types (Fig. 3; S2/S3 ratio in Table 2).

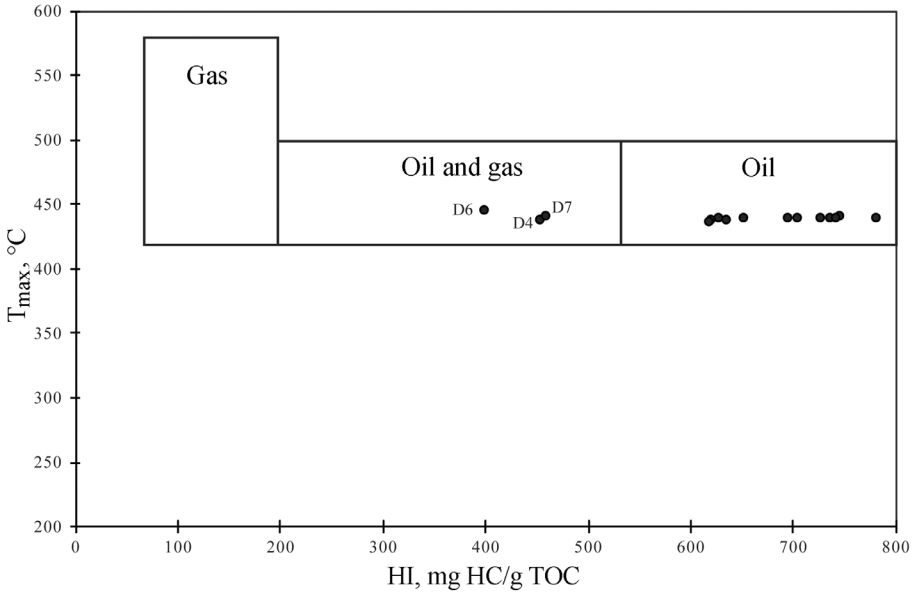

Fig. 4. Plot T_{max} vs HI.

4.2.3. Molecular composition of organic matter

4.2.3.1. Sources of organic matter

The OM source parameters of analysed samples were calculated based on distributions and abundances of *n*-alkanes, isoprenoids, steranes and terpanes (Fig. 5; Table 3). Biomarker distributions shown in Figure 5 also suggest certain differences between sample D16 and the rest of the samples.

The *n*-alkanes are identified in the range of C_{15}–C_{35}. The distribution of *n*-alkanes is characterised by the dominance of *n*-C_{27}, *n*-C_{29}, *n*-C_{31} and/or *n*-C_{21}, *n*-C_{22}, *n*-C_{23} alkane homologues (Fig. 5a–b). The long-chain odd *n*-alkane homologues (C_{27}–C_{33}) commonly indicate contribution of higher plants, while mid-chain *n*-alkanes (C_{21}–C_{25}) are derived from bacteria, algae, aquatic macrophytes and sphagnum. Short-chain *n*-alkanes (< C_{20}) originate from algae and bacteria.

The values of the terrigenous/aquatic ratio (TAR) in the analysed samples (Table 3) are relatively high and could be indicative of a higher terrigenous input from the surrounding watershed.

However, certain non-marine algae such as *Botryococcus braunii* race A could also contribute to C_{27}–C_{31} *n*-alkanes [29]. In earlier research it has been found that OM in the Aleksinac oil shale deposit predominantly originated from algae represented by lamalginite, whose precursor can be identified as lacustrine green algae *Botryococcus braunii* and *Pediastrum* [3, 12]. Moreover, Rock-Eval data suggest kerogen types I and/or II (Fig. 3; Table 2). Therefore, it can be assumed that the green unicellular microalga, *Botryococcus braunii* race A, was one of the sources of the OM in the investigated samples. Considering the low maturity of OM, the CPI values (Table 3) do not reflect a high input of land plant material, which is consistent with Rock-Eval data (Table 2).

The major isoprenoid alkanes in the analysed samples are pristane (Pr) and phytane (Ph) (Fig. 5a–b). In some samples regular isoprenoid alkanes C_{16}, C_{18}, C_{21}, C_{25} and irregular C_{30} isoprenoid (squalane) are also present in low abundance. The presence of C_{16} and C_{18} regular isoprenoid alkanes is indicative of algal input [30]. The main precursors of C_{21}–C_{30} regular isoprenoid alkanes are lipids of haloalkaliphilic archaea [8, 31]. β-Carotane is identified in all samples. Carotenoids are tetraterpenoid organic pigments which are widely distributed in living organisms such as algae (particularly *Dunaliella salina*), bacteria and higher plants [8].

The distribution of steranes (Fig. 5c–d) is dominated by regular C_{27}–C_{29} steranes with the biogenic 5α(H)14α(H)17α(H)20R-configuration. Steranes with 5α(H)14α(H)17α(H)20S-configuration, represented only by C_{29} homologue, and low molecular weight steranes (C_{21}–C_{26}) are present in low amount. 4-Methylsteranes C_{28}–C_{30} (*m/z* 231) were only identified in sample D16.

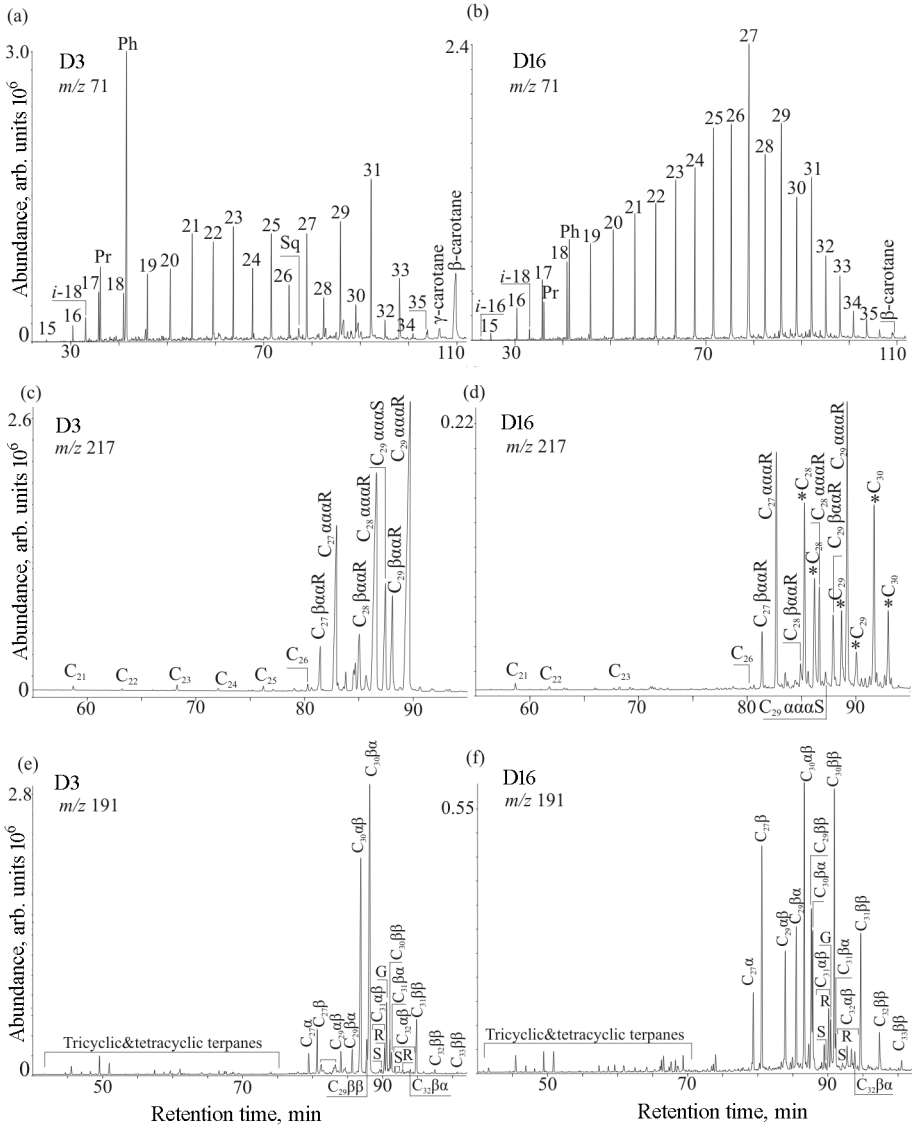

Fig. 5. GC-MS chromatograms of *n*-alkanes and isoprenoids (a, b), steranes (c, d) and terpanes (e, f) of representative samples D3 and D16.

n-Alkanes are labeled according to their carbon number; Pr – pristane; Ph – phytane; *i*-18 – C_{18} regular isoprenoid; Sq – squalane; C_{21}–C_{26}–C_{21}–C_{26} steranes with 14α(H)17α(H) configuration; βαα and ααα designate 5β(H)14α(H)17α(H) and 5α(H)14α(H)17α(H) configurations in steranes; S and R designate configuration at C-20 in steranes; * – C_{28}–C_{30}-4-methylsteranes; α and β designate configuration at C-17 in C_{27} hopanes; αβ, βα and ββ designate configurations at C-17 and C-21 in C_{29}–C_{33} hopanes; S and R designate configuration at C-22 in C_{31}–C_{32} hopanes; G – gammacerane. (The abbreviation used: arb. – arbitrary.)

Table 3. Values of biomarker parameters

Sample No.	TAR	CPI (C_{15}–C_{35})	%C_{27}	%C_{28}	%C_{29}	S/H	C_{29}ααα 20S/(20S + 20R)	C_{31}αβ 22S/(22S + 22R)	C_{30}βα/C_{30}αβ	Rc, %	Pr/Ph	Pr/n-C_{17}	Ph/n-C_{18}	β-Car	GI	C_{26}TT/C_{25}TT	C_{31}αβ 22R/C_{30}αβ
D1	5.86	1.16	38.93	26.95	34.12	3.40	0.11	0.24	1.71	0.39	0.16	0.87	2.95	3.19	2.51	2.25	0.17
D2	4.45	2.26	16.76	34.42	48.82	4.90	0.18	0.14	1.42	0.44	0.16	1.68	7.99	9.85	2.26	2.11	0.20
D3	5.07	2.27	16.88	35.89	47.23	4.19	0.18	0.16	1.44	0.44	0.15	1.71	10.04	12.68	2.05	1.89	0.09
D4	6.28	1.80	17.72	36.00	46.28	0.80	0.18	0.22	1.02	0.44	0.32	0.74	0.04	3.61	2.51	1.57	0.06
D5	4.35	1.92	10.75	34.38	54.87	1.60	0.19	0.25	0.56	0.44	0.43	0.62	0.90	2.34	2.18	2.13	0.13
D6	3.30	2.00	10.94	39.66	49.40	2.08	0.15	0.25	0.71	0.42	0.20	0.51	2.70	1.79	2.38	1.69	0.04
D7	6.95	1.50	26.52	31.87	41.62	1.69	0.13	0.21	1.59	0.41	0.31	0.72	1.57	3.58	2.05	1.53	0.07
D8	2.58	2.48	12.97	39.41	47.62	3.43	0.16	0.17	0.95	0.42	0.24	1.22	12.55	6.35	1.01	2.12	0.08
D9	4.14	1.87	35.85	29.32	34.83	2.87	0.13	0.23	1.67	0.40	0.17	0.65	2.63	2.76	2.58	2.24	0.18
D10	5.32	2.99	22.15	35.59	42.26	1.90	0.10	0.15	1.69	0.39	0.25	1.09	2.73	7.11	1.13	2.07	0.21
D11	6.46	2.85	33.10	27.88	39.02	4.78	0.11	0.30	1.56	0.38	0.30	0.88	1.99	6.84	1.24	2.18	0.08
D12	7.47	2.20	18.81	36.61	44.58	4.15	0.11	0.15	1.88	0.39	0.30	3.38	8.72	12.33	1.03	2.27	0.10
D13	2.69	1.87	20.07	42.29	37.65	5.29	0.14	0.11	1.93	0.41	0.32	4.02	16.99	9.36	1.09	2.67	0.12
D14	7.98	1.94	21.55	33.86	44.59	2.71	0.13	0.14	1.87	0.40	0.21	1.14	4.33	2.68	1.62	2.29	0.26
D15	4.13	1.19	20.32	37.70	41.98	2.47	0.11	0.16	1.82	0.38	0.38	0.79	1.42	8.43	1.14	1.67	0.20
D16	7.76	1.37	32.74	20.80	46.47	0.50	0.07	0.12	0.43	0.36	0.36	0.68	1.42	0.83	1.78	2.18	0.23

Note: TAR – terrigenous/aquatic ratio = (*n*-C_{27} + *n*-C_{29} + *n*-C_{31})/(*n*-C_{15} + *n*-C_{17} + *n*-C_{19}); CPI – Carbon Preference Index, CPI (C_{15}–C_{35}) = ½ × [Σodd(*n*-C_{15}–*n*-C_{35})/Σeven(*n*-C_{14}–*n*-C_{34}) + Σodd(*n*-C_{15}–*n*-C_{35})/Σeven(*n*-C_{16}–*n*-C_{36})]; %C_{27} – C_{27}/(C_{27} + C_{28} + C_{29}) of 5α(H)14α(H)17α(H)20R-steranes; %C_{28} – C_{28}/(C_{27} + C_{28} + C_{29}) of 5α(H)14α(H)17α(H)20R-steranes; %C_{29} – C_{29}/(C_{27} + C_{28}+C_{29}) of 5α(H)14α(H)17α(H)20R-steranes; S/H = [Σ(C_{27}–C_{29}) 5α(H)14α(H)17α(H)(20S + 20R)-steranes]/[Σ(C_{29}–C_{33}) 17α(H)21β(H)-hopanes]; C_{29}ααα 20S/(20S + 20R) = C_{29} 5α(H)14α(H)17α(H)20S-sterane/C_{29} 5α(H)14α(H)17α(H)(20S + 20R)-steranes; C_{31}αβ 22S/(22S + 22R) = C_{31} 17α(H)21β(H)22(S)-homohopane/C_{31} 17α(H)21β(H)(22S + 22R)-homohopanes; C_{30}βα/C_{30}αβ = C_{30} 17β(H)21α(H)-moretane/C_{30} 17α(H)21β(H)-hopane; Rc – calculated vitrinite reflectance = 0.49 × C_{29}ααα 20S/20R + 0.33; Pr/Ph = pristane/phytane; β-Car = β-carotane/Σ of all peaks in Total Ion Current (TIC) of saturated fraction; GI = gammacerane × 10/(gammacerane + C_{30} 17α(H)21β(H)-hopane); C_{26}TT/C_{25}TT = C_{26}-tricyclic terpane/C_{25}-tricyclic terpane; C_{31}αβ 22R/C_{30}αβ = C_{31} 17α(H)21β(H)22(R)-homohopane/C_{30} 17α(H)21β(H)-hopane.

The majority of the samples are characterised by the dominance of C_{29} followed by C_{28} regular sterane, or in some samples (D11, D16) by C_{27} regular sterane. The C_{29} regular steranes originate from sterols of higher plants, as well as from cyanobacterial and algal biolipid sterols [32]. Combining this result with *n*-alkane distribution (Fig. 5a–b), parameters (TAR, CPI; Table 3) and kerogen types (Fig. 3; Table 2), the predominance of C_{29} sterane probably indicates a strong contribution of aquatic organisms such as green and brown algae (consistent with the contribution of *Botryococcus braunii* race A and *Pediastrum*), and some influence of higher plants OM.

The exact origin of C_{21}–C_{25} steranes remains unclear and they are often associated with microbially mediated diagenetic processes in the specific depositional environment, whereas diatoms are considered as the main pre-cursors of C_{26} steranes [8]. C_{28}–C_{30} 4-methylsteranes, which were exclusively identified in sample D16 (Fig. 5d), are specific for dinoflagellates, certain bacteria and prymnesiophyte microalgae, restricted to marine or lacustrine environments [8, 33].

The terpane distribution is characterised by the dominance of pentacyclic terpanes, i.e. hopanes, and a relatively low abundance of tricyclic (C_{19}–C_{30}) and tetracyclic (C_{24}) terpanes (Fig. 5e–f). The hopane distribution is represented by C_{27} 17β(H)- and 17α(H)-trisnorhopanes, C_{29}–C_{32} 17β(H)21α(H)-moretanes and C_{29}–C_{32} 17α(H)21β(H)-hopanes, as well as by C_{29}–C_{33} hopanes with the biogenic 17β(H)21β(H) configuration which is typical for immature OM. Prokaryotes are considered as the main biological precursors of geo-hopanes [34]. More abundant C_{29} hopanes in sample D16 (Fig. 5f) are consistent with carbonate source (Table 1) [8]. The tricyclic terpanes, present in low abundance in all samples, imply a microbial or algal origin [8]. The presence of gammacerane in all samples (Table 3) is indicative of bacterivorous ciliates, which occur in stratified water columns [8].

The sterane/hopane ratio (S/H) reflects the input of eukaryotic (algae and higher plants) vs prokaryotic organisms to OM [8]. All samples, with the exception of D4 and D16, have the S/H > 1. Considering the previous discussion, this result can be attributed to the dominant algal input to OM relative to bacteria (Table 3).

4.2.3.2. Maturity of organic matter

The parameters, C_{29}ααα 20S/(20S + 20R) sterane ratio, C_{31}αβ 22S/(22S + 22R) homohopane ratio and C_{30}βα/C_{30}αβ ratio, were used to estimate the maturity of organic matter. The values of these maturity parameters (Table 3) are very far from equilibrium values (Table 4) [8] showing that the OM of all samples is immature, which is consistent with the previously discussed parameters (S1, Tmax and PI; Table 2). Based on the sterane maturity ratio (Rc = 0.49 × C_{29}ααα 20S/20R + 0.33) [35], the calculated vitrinite reflectance ranging from 0.36 to 0.44% (Table 3) is in accordance with the measured vitrinite reflectance in the Aleksinac oil shale (Rr = 0.41%) [12] and main coal seam (Rr = 0.44%) [3].

4.3. Depositional environment

The absence of C_{30} 4-desmethylsteranes (24-*n*-propylcholestanes), as well as the C_{26}/C_{25} tryciclic terpane ratio > 1 and $C_{31}\alpha\beta$ 22R/$C_{30}\alpha\beta$ hopane ratio < 0.25 (Table 3) in all samples indicate lacustrine depositional settings [8].

The values of Pr/Ph < 1 generally characterised a reducing depositional environment [36]. However, low Pr/Ph ratio (< 0.8) was also reported in hypersaline environments [37]. The biomarker composition showed that there were no indications of hypersalinity (e.g. C_{21}–C_{25} regular isoprenoids are absent or are present in traces only, 8-methyl-2-methyl-2-(4,8,12-trimethyltridecyl) chroman is absent, extended homohopanes above C_{31} are not prominent in hopane distribution, C_{35} homohopane is absent) [8]. Therefore, the Pr/Ph ratio < 0.4 in all samples (Table 3) implies sedimentation under reducing conditions, which contributed to the good preservation of algal OM.

The presence of β-carotane in all samples (Fig. 5a–b), being at the same the most abundant compound in the total saturated fraction of several samples (Table 3), is a further confirmation of deposition of OM in a reducing environment. β-Carotane is commonly interpreted as a specific indicator of anoxic lacustrine, or highly restricted marine environments [8, 38]. The lower abundance of β-carotane in sample D16 can be attributed to the non-deep water column (less reducing conditions) and high sulphur content (Table 2). Namely, the double bonds in β-carotene, the main precursor of β-carotane, can react with sulphur species, becoming part of a sulphur cross-linked system [39], while in low-sulphur anoxic lacustrine systems (samples D1–D15) β-carotene is reduced to β-carotane. Such lacustrine systems are usually associated with algal-rich OM, showing high S/H ratio [40], as in the case of D1–D15 samples (Table 3).

Gammacerane, identified in all samples, is specific for water-column stratification, which commonly resulted from salinity at depth or temperature gradients [41]. The presence of both gammacerane and β-carotane represents the confirmation of water-column stratification and anoxic conditions at depth.

As previously mentioned, sample D16 mostly differs from the other samples in mineral composition, TOC amount and biomarker patterns (Tables 1–3). Carbonates are predominant minerals, aragonite, bassanite and series of 4-methylsteranes were identified exclusively in this sample, whereas minerals of feldspar and zeolite groups, as well as dolomite and Ca-rich dolomite (or ankerite) were absent. These results indicate sedimentation in a calm alkaline environment (predominance of carbonates) under warm climate conditions (presence of bassanite), which contributed to water column stratification and the preservation of OM. The S/H ratio < 1 implies the prevalence of prokaryotic OM over algal, which may result from a shallow water column, consistent with an elevated temperature and lower amount of β-carotane. The enrichment of sulphur is probably the result of an alkaline environment permitting sulphate-reducing bacteria to thrive [42]. Abundant 4-methylsteranes and their distribution, which shows the trend

$C_{30} \approx C_{28} > C_{29}$ (Fig. 5d), indicate a brackish lacustrine environment [39], supported also by the Corg/TS ratio of approximately 5 (Table 2) [43]. The obtained result can be attributed to intense tectonic movements during the Miocene, which have caused changes in deposition pattern. As a result, there was a hiatus in the area of the Aleksinac deposit during the Middle Miocene (Fig. 2), but also minor marine ingression(s) during the Lower Miocene. Regional tilting affected an area of the seaway that connected the Paratethys Sea to the north, and caused a sudden marine inflow to the east, at the time of deposition of sediments represented by sample D16.

Samples D1–D15 contain a considerably lower amount of TOC than sample D16 (Table 2). These samples have notably higher contents of feldspars derived mostly from the terrigenous fraction of sedimentary rocks and lower contents of carbonate minerals in comparison to sample D16 (Table 1). This change, probably also induced by tectonic movements, can be related to the contribution of clastic material coupled with the nutrients-rich freshwater influx (resulting in increase of Corg/TS ratio > 10; Table 2) that supported high bioproductivity, which led to the formation of algal (*Botryococcus braunii* and *Pediastrum*) organic-rich sediments. Moreover, a slight rise of the water column and its stratification supported by warm climate [5] contributed to anoxic conditions at depth, which favoured OM preservation. Besides, the influx of fresh water into the basin which induced increased transport of clastic material into the basin, probably led to high sedimentation rates. Minor differences in biomarker distribution between samples D1–D15 (Table 3) can be attributed to slight variations in water column level (redox conditions) and contribution of clastic material/ allochtonous biomass of land plants, particularly in the samples with lower hydrocarbon generative potential (D4, D6 and D7).

4.4. Simulation of catagenesis phase by pyrolysis

The generative potential of samples was also investigated using conventional pyrolysis [10]. Pyrolysis was performed on bitumen-free samples D13 and D16. Sample D13 has the highest HI, whereas sample D16 is characterised by the highest TOC (Table 2). Moreover, as already discussed, sample D16 mostly differs from the other samples in several aspects (Tables 1–3; Fig. 5). By pyrolysis, bitumen-free D13 and D16 samples generated a total liquid pyrolysate of 43900 and 39019 ppm, and hydrocarbons of 1790 and 2255 ppm, respectively (Table 4). The yields are consistent with those of a source rock with very good potential [25] and support the assumption derived from elemental analysis and Rock-Eval pyrolysis of the initial samples (Table 2). Therefore it can be assumed that OM content and type primarily determined the generative potential of OS, whereas the observed differences in mineral composition between D13 and D16 samples (Table 1) had a low impact.

Both pyrolysates have similar *n*-alkane distributions, in which *n*-alkanes C_{16}–C_{20} are predominant (Fig. 6a; Table 4). The CPI values for the pyro-

Table 4.Values of organic geochemical parameters in liquid pyrolysates

Sample No.	Yield of liquid pyrolysate[1], ppm	Yield of HC, ppm	CPI(C_{15}–C_{35})	%C_{27}	%C_{28}	%C_{29}	C_{31}αβ 22S/(22S + 22R)	C_{29}ααα 20S/(20S + 20R)	C_{29} αββ/(αββ + ααα)	Rc, %
PyD13	43900	1790	1.03	30.20	33.62	36.18	0.55	0.47	0.50	0.76
PyD16	39019	2255	1.06	34.60	30.22	35.18	0.54	0.55	0.57	0.92
E.V.	/	/	/	/	/	/	0.57–0.62	0.52–0.55	0.67–0.71	/

Note: [1] – relative to bitumen-free samples;
C_{29} αββ/(αββ + ααα) = C_{29} 5α(H)14β(H)17β(H)20R-sterane/(C_{29} 5α(H)14β(H)17β(H)20R + C_{29} 5α(H)14α(H)17α(H)20R)-steranes;
E.V. – equilibrium values [8]; for other abbreviations see the legend of Table 3.

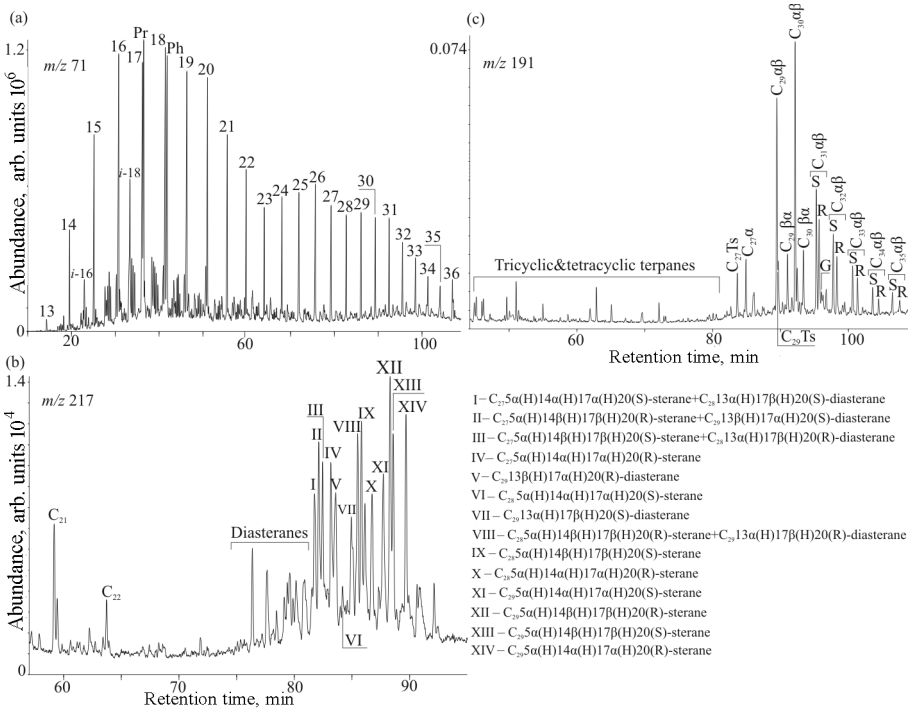

Fig. 6. GC-MS chromatograms of *n*-alkanes (m/z 71; a), steranes (m/z 217; b) and terpanes (m/z 191; c) of the liquid pyrolysate of sample D16. *i*-16 – C16 regular isoprenoid; C_{21} and C_{22}–C_{21} and C_{22} 14α(H)17α(H) + 14β(H)17β(H)-steranes; C_{27}Ts – C_{27} 18α(H)-22,29,30-trisnorneohopane; C_{29}Ts – C_{29} 18α(H)-30-norneohopane; for other peak assignments, see the legend of Fig. 5. (The abbreviation used: arb. – arbitrary.)

lysates are close to 1, which is typical of a mature oil distribution (Table 4). An increase in the contents of C_{27} steranes in both pyrolysates and content of C_{28} sterane in pyrolysate of D16 (Tables 3, 4) in comparison to initial samples is consistent with OM type.

The sterane and hopane distributions in pyrolysates are typical for oils (Fig. 6b–c), which shows that catagenesis was simulated successfully by pyrolysis. Values for $C_{31}\alpha\beta$ 22S/(22S + 22R)-homohopanes (Table 4) show that equilibrium had been achieved in both pyrolysates, which indicates maturity > 0.60% Rr. Sterane parameters $C_{29}\alpha\alpha\alpha$ 20S/(20S + 20R) and $C_{29}\alpha\beta\beta/(\alpha\beta\beta + \alpha\alpha\alpha)$, which are more applicable at higher maturity levels than $C_{31}\alpha\beta$ 22S/(22S+22R) ratio, have slightly lower values in pyrolysates than proposed equilibrium values (Table 4). This confirms that by pyrolysis maturity corresponding to the beginning of the main stage of oil generation was achieved. It is also documented by calculated vitrinite reflectance based on sterane maturity ratio (Rc) [35] in pyrolysates, having the values of 0.76 and 0.92 %, respectively (Table 4). Moreover, this result indicates a notable increase in OM maturity in comparison to initial samples, which showed Rr and Rc of ca. 0.40%.

5. Conclusions

The origin, depositional environment, maturity and hydrocarbon generative potential of the organic matter of new oil shale samples from the outcrops of the upper layer in the Dubrava area, Aleksinac basin, Serbia, were evaluated.

The mineral part of analysed samples is composed of clays, feldspars, carbonates, analcime, natrolite, quartz and bassanite. Most of the samples have similar mineral compositions with predominance of clay and feldspar minerals. Three samples are characterised by an elevated content of carbonates. Among them, sample D16 has a notable prevalence of this mineral group. D16 also demonstrates certain differences in biomarker distribution and has a considerably higher TOC content.

In most samples organic matter consists predominantly of type I and II kerogens, showing high oil generative potential. Three samples (D4, D6 and D7) containing type II kerogen with a certain input of type III kerogen demonstrate potential to produce both, oil and gas. The organic matter of all samples is immature and corresponds to the vitrinite reflectance of ca. 0.40%.

Biomarker patterns along with Rock-Eval data indicated a notable contribution of aquatic organisms such as green (e.g. *Botryococcus braunii* race A) and brown algae and bacteria with some influence of higher plants OM.

The organic matter was deposited in a reducing lacustrine alkaline brackish to freshwater environment under warm climate conditions. Having started in a shallow calm carbonate alkaline brackish environment, deposition of organic-rich oil shales, represented by sample D16, resulted from

intense tectonic movements which caused marine inflow from the seaway connected to the Paratethys Sea. Through time, change in depositional environment (samples D15–D1), probably also induced by tectonic movements, has occurred. That change was expressed by the influx of fresh water rich in nutrients that supported high bioproductivity, coupled with contribution of clastic material which resulted in high sedimentation rates and lowering of TOC. Minor differences in mineral composition and biomarker distribution between samples D1–D15 can be attributed to variations in water column level (redox conditions) and contribution of clastic material/ allochtonous biomass of land plants, particularly in the samples with lower hydrocarbon generative potential (D4, D6 and D7).

Conventional pyrolytic experiments confirmed that these sediments at the catagenetic stage could be a significant source of liquid hydrocarbons.

Acknowledgments

The study was supported by the Ministry of Education, Science and Technological Development of the Republic of Serbia (Project No. 176006). PDF-2 was used with permission from the International Centre for Diffraction Data. We are also grateful to Dr. Tarmo Kiipli, an anonymous reviewer, Executive Editor, Meelika Nõmme and Editor, Riina Süld.

REFERENCES

1. Ercegovac, M., Grgurović, D., Bajc, S., Vitorović, D. Oil shale in Serbia: geological and chemical-technological investigations, actual problems of exploration and feasibility studies. In: *Mineral Material Complex of Serbia and Montenegro at the Crossings of Two Millenniums* (Vujić, S., ed.). Margo-Art, Belgrade, 2003, 368–378 (in Serbian, with English abstract).
2. Jelenković, R., Kostić, A., Životić, D., Ercegovac, M. Mineral resources of Serbia. *Geol. Carpath.*, 2008, **59**(4), 345–361.
3. Ercegovac, M., Vitorović, D., Kostić, A., Životić, D., Jovančićević, B. Geology and Geochemistry of the Aleksinac oil shale deposit (Serbia). In: *Book of Abstracts Joint 61st ICCP/26th TSOP Meeting "Advances in Organic Petrology and Organic Geochemistry"*, September 19–26, 2009, Gramado, Brazil, P13, p. 6.
4. Skala, D., Bastić, M., Jovanović, J., Rahimian, I. Pyrolysis of oil shale in a microretorting unit. *Fuel*, 1993, **72**(6), 829–835.
5. Obradović, J., Djurdjević-Colson, J., Vasić, N. Phytogenic lacustrine sedimentation – oil shales in Neogene from Serbia, Yugoslavia. *J. Paleolimnol.*, 1997, **18**(4), 351–364.
6. Čokorilo, V., Lilić, N., Purga, J., Milisavljević, V. Oil shale potential in Serbia. *Oil Shale*, 2009, **26**(4), 451–462.
7. Tissot, B. P., Welte, D. H. *Petroleum Formation and Occurrence, 2nd ed*. Springer-Verlag, Heidelberg, 1984.

8. Peters, K. E., Walters, C. C., Moldowan, J. M. *The Biomarker Guide, Vol. 2: Biomarkers and Isotopes in Petroleum Exploration and Earth History, Second edition.* Cambridge University Press, Cambridge, 2005.
9. Huizinga, B. J., Aizenshtat, Z. A., Peters, K. E. Programmed pyrolysis-gas chromatography of artificially matured Green River kerogen. *Energ. Fuel.*, 1988, **2**, 74–81.
10. Stojanović, K., Šajnović, A., Sabo, T. J., Golovko, A., Jovančićević, B. Pyrolysis and catalyzed pyrolysis in the investigation of a Neogene shale potential from Valjevo-Mionica basin, Serbia. *Energ. Fuel.*, 2010, **24**(8), 4357–4368.
11. Petrović, M. *Reserve Report for the Aleksinac Oil Shale – "Dubrava" Field*. JP PEU, Resavica, 2012 (in Serbian).
12. Ercegovac, M. *Geology of Oil Shale*. Građevinska knjiga, Belgrade, 1990 (in Serbian).
13. Perunović, T., Stojanović, K., Simić, V., Kašanin-Grubin, M., Šajnović, A., Erić. V., Schwarzbauer, J., Vasić, N., Jovančićević, B., Brčeski, I. Organic geochemical study of the lower Miocene Kremna basin, Serbia. *Ann. Soc. Geol. Pol.*, 2014, **84**(3), 185–212.
14. Vuković, N., Životić, D., Mendonça Filho, J. G., Kravić-Stevović, T., Hámor-Vidó, M., Mendonça, J. O., Stojanović, K. The assessment of maturation changes of humic coal organic matter – insights from closed-system pyrolysis experiments. *Int. J. Coal Geol.*, 2016, **154–155**, 213–239.
15. Kabekkodu, S. N. (ed.). *PDF-2 Release 2008.* International Centre for Diffraction Data: Newtown Square, PA, 2008.
16. Rao, C. P. *Modern Carbonates, Tropical, Temperate, Polar: Introduction to Sedimentology and Geochemistry.* University of Tasmania, Hobart, Tasmania, 1996.
17. Müller, G., Irion, G., Förstner, U. Formation and diagenesis of inorganic Ca-Mg carbonates in the lacustrine environment. *Naturwissenschaften*, 1972, **59**(4), 158–164.
18. Guo, L., Jiang, Z., Liang, C. Mineralogy and shale gas potential of Lower Silurian organic-rich shale at the southeastern margin of Sichuan Basin, South China. *Oil Shale*, 2016, **33**(1), 1–17.
19. Remy, R. R., Ferrell, R. E. Distribution and origin of analcime in marginal lacustrine mudstones of the Green River Formation, south-central Uinta Basin, Utah. *Clays Clay Miner.*, 1989, **37**(5), 419–432.
20. Kašanin-Grubin, M. *Sedimentology of the Oil Shales Series of the Aleksinac Basin*. Master thesis, University of Belgrade, Belgrade, 1996 (in Serbian, with English abstract).
21. Harrison, T. N. Experimental VNIR reflectance spectroscopy of gypsum dehydration: Investigating the gypsum to bassanite transition. *Am. Mineral.*, 2012, **97**(4), 598–609.
22. Hunt, J. M. *Petroleum Geochemistry and Geology*, *2nd ed*. W. H. Freeman and Company, New York, 1996.
23. Peters, K. E. Guidelines for evaluating petroleum source rock using programmed pyrolysis. *AAPG Bull.*, 1986, **70**(3), 318–329.
24. Peters, K. E., Cassa, M. R. Applied source rock geochemistry. In: *The Petroleum System - From Source to Trap* (Magoon, L. B., Dow, W. G., eds.), AAPG Memoir 60. Tulsa, 1994, 93–120.

25. Peters, K. E., Walters, C. C., Moldowan, J. M. *The Biomarker Guide, Vol. 1: Biomarkers and Isotopes in the Environment and Human History, Second edition*. Cambridge University Press, Cambridge, 2005.
26. Espitalié, J., Deroo, G., Marquis, F. La pyrolyse Rock-Eval et ses applications. Deuxième Partie. *Rev. I. Fr. Petrol.*, 1985, **40**(6), 755–784 (in French, with English abstract).
27. Bordenave, M. L., Espitalié, J., Leplat, P., Oudin, J. L., Vandenbroucke, M. Screening techniques for source rock evaluation. In: *Applied Petroleum Geochemistry* (Bordenave, M. L., ed.). Éditions Technip, Paris, 1993, 217–278.
28. Dyman, T. S., Palacas, J. G., Tysdal, R. G., Perry, W. J., Pawlewicz, M. J. Source rock potential of middle Cretaceous rocks in Southwestern Montana. *AAPG Bull*., 1996, **80**(8), 1177–1184.
29. Moldowan, J. M., Seifert, W. K., Gallegos, E. J. Relationship between petroleum composition and depositional environment of petroleum source rocks. *AAPG Bull.*, 1985, **69**(8), 1255–1268.
30. Volkman, J. K., Zhang, Z., Xie, X., Qin, J., Borjigin, T. Biomarker evidence for *Botryococcus* and a methane cycle in the Eocene Huadian oil shale, NE China. *Org. Geochem.*, 2015, **78**, 121–134.
31. De Rosa, M., Gambacorta, A., Gliozzi, A. Structure, biosynthesis, and physicochemical properties of archaebacterial lipids. *Microbiol. Rev.*, 1986, **50**(1), 70–80.
32. Volkman, J. K. A review of sterol markers for marine and terrigenous organic matter. *Org. Geochem*., 1986, **9**(2), 83–99.
33. Wolff, G. A., Lamb, N. A., Maxwell, J. R. The origin and fate of 4-methyl steroid hydrocarbons. 1. Diagenesis of 4-methyl sterenes. *Geochim. Cosmochim. Ac.*, 1986, **50**(3), 335–342.
34. Ourisson, G., Albrecht, P., Rohmer, M. The hopanoids: palaeochemistry and biochemistry of a group of natural products. *Pure Appl. Chem.*, 1979, **51**(4), 709–729.
35. Sofer, Z., Regan, D. R., Muller, D. S. Sterane isomerization ratios of oils as maturity indicators and their use as an exploration tool, Neuquen Basin, Argentina. *Book of Proceedings*, XII Geological Congress, Buenos Aires, Argentina, 1993, 407–411.
36. Didyk, B. M., Simoneit, B. R. T., Brassell, S. C., Eglinton, G. Organic geochemical indicators of palaeoenvironmental conditions of sedimentation. *Nature*, 1978, **272**, 216–222.
37. ten Haven, H. L., de Leeuw, J. W., Rullkötter, J., Sinninghe Damsté, J. S. Restricted utility of the pristane/phytane ratio as a palaeoenvironmental indicator. *Nature*, 1987, **330**, 641–643.
38. Fu, J., Sheng, G., Xu, J., Eglinton, G., Gowar, A. P., Jia, R., Fan, S., Peng, P. Application of biological markers in the assessment of paleoenvironments of Chinese non-marine sediments. *Org. Geochem.*, 1990, **16**(4–6), 769–779.
39. Adam, P., Schmid, J. C., Mycke, B., Strazielle, C., Connan, J., Huc, A., Riva, A., Albrecht, P. Structural investigation of nonpolar sulfur cross-linked macromolecules in petroleum. *Geochim. Cosmochim. Ac.*, 1993, **57**(14), 3395–3419.
40. Peters, K. E., Cunningham, A. E., Walters, C. C., Jiang, J., Fan, Z. Petroleum systems in the Jiangling-Dangyang area, Jianghan Basin, China. *Org. Geochem.*, 1996, **24**(10–11), 1035–1060.

41. Sinninghe Damsté, J. S., Kenig, F., Koopmans, M. P., Köster, J., Schouten, S., Hayes, J. M., de Leeuw, J. W. Evidence for gammacerane as an indicator of water column stratification. *Geochim. Cosmochim. Ac.*, 1995, **59**(9), 1895–1900.
42. Casagrande, D. J. Sulphur in peat and coal. In: *Coal and Coal-Bearing Strata: Recent Advances* (Scott, A. C., ed.). Geol. Soc. Spec. Publ. **32**, London, 1987, 87–105.
43. Berner, R. A., Raiswell, R. C/S method for distinguishing freshwater from marine sedimentary rocks. *Geology*, 1984, **12**(6), 365–368.

Presented by E. Reinsalu
Received September 25, 2016